Object Slippage Prevention using Different Control Strategies

Pavel Dzitac[1], Abdul Md Mazid[2], Guy Littlefair[1] and Ashwin Polishetty[1]
[1]*School of Engineering, Deakin University, Geelong, Australia*
[2]*Department of Engineering, Macquarie University, Sydney, Australia*

Keywords: Robotic Grasping, Slippage Sensing, Tangential Force Sensing, Slippage Detection, Slippage Prevention, Incipient Slippage, Grasp Force Estimation, Grasp Force Control.

Abstract: This paper presents experimental results obtained using a friction-based slippage and tangential force sensing device that has been developed for the purpose of reliable object slippage prevention during robotic manipulation. The experimental results obtained demonstrate that the developed slippage sensing strategy is rugged and reliable even in its current "rough prototype" state of development. This work has the potential to yield a low cost and highly customisable slippage and tangential force sensing device for a variety of robotic object grasping and manipulation applications. It is envisaged that the work presented here will be beneficial to researchers in the area of object slippage prevention.

1 INTRODUCTION

Reliable grasping and manipulation incorporates control decisions that perform better than the basic "grasp and hold tight" strategies. Adequate grasp force control is essential to reliable and safe manipulation; it improves robot's chances to manipulate objects autonomously close to optimum conditions on the first attempt.

Slippage takes place in two stages: incipient slippage and bulk or gross slippage (Tremblay and Cutkosky, 1993). It is characterised by a mechanical behaviour known as "stick-slip" that results in vibration and is present during relative motion between two surfaces in contact (Bowden and Tabor, 1986). In order to prevent slippage it is necessary to predict what researchers call pre-slip (Petchartee and Monkman, 2007) or incipient slip (Bowden and Tabor, 1986), (Mingrino et. al, 1994, Canepa et al., 1994, Pelossof et al., 2004), the tell-tale sign that slippage is about to occur. Predictive measures such as incipient slip detection have been used by researchers to control slippage during object manipulation (Canepa et al., 1994, Pelossof et al., 2004, Dubey and Crowder, 2006, Watanabe and Obinata, 2007).

The stick-slip vibration frequency and amplitude are dependent on many factors and are not a constant behaviour during slippage under all conditions; vibration frequency and amplitude vary with object materials, different surface conditions and speed (Bowden and Tabor, 1986, Abdo et al., 2009). Stick-slip can be reduced under certain conditions by applying a particular range of vibration frequencies at specific amplitudes to the system that produces the stick-slip induced vibration (Abdo et al., 2009). It may also be challenging to distinguish stick-slip vibration from background noise. Therefore, it could be concluded that stick-slip is not an ideal source for generic incipient slippage detection, but it is a mechanical behaviour by which most slippage events can be detected using vibration detection techniques.

Researchers have developed many tactile sensors intended for grasp force and slippage control (Russel, 1990, Choi et al., 2005, Rossiter and Mukai, 2005, Dahiya et al., 2010). Industrial robotics applications require sensors that can handle significant loads; a load of 50 N is towards the low end on the load scale. Therefore load bearing capacity and the ability to maintain sensitivity at maximum load are important criteria that determine the suitability of a sensing technology for industrial robotics applications.

This paper presents experimental results obtained with the latest friction-based slippage and tangential force sensing prototype, in conjunction with various slippage detection and prevention strategies.

The working principle of the friction-based slippage sensing device is described in (Dzitac and

Dzitac, P., Mazid, A., Littlefair, G. and Polishetty, A.
Object Slippage Prevention using Different Control Strategies.
DOI: 10.5220/0006003505590566
In *Proceedings of the 13th International Conference on Informatics in Control, Automation and Robotics (ICINCO 2016) - Volume 1*, pages 559-566
ISBN: 978-989-758-198-4

Mazid, 2012), and is briefly summarised here to facilitate understanding.

2 FRICTION-BASED SLIPPAGE SENSING

The slippage sensing device relies on friction between two sets of friction surfaces: one at the roller-shaft interface, and the other at the roller-object interface (Figure 1).

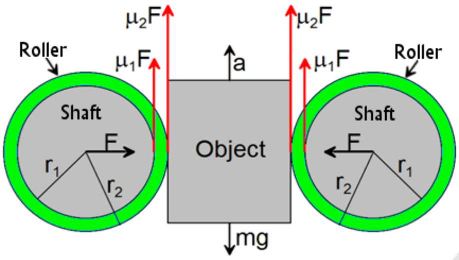

Figure 1: Friction-based parallel jaw gripper concept with rollers on support shaft.

When the applied grasp force to the object is insufficient, the roller slips on its support shaft, but still rolls on the surface of the manipulated object. This allows the static coefficient of friction to be maintained at the roller-object interface. Therefore, this design incorporates the following benefits.

- Slippage starts at the roller-shaft interface well before slippage at the gripper-object interface, which facilitates object slippage prevention;
- The static and dynamic coefficients of friction at the roller-shaft interface are known in advance, which allows adequate grasp force application when object mass is known.

In Figure 1 the friction force between the roller and its support shaft is given by

$$F_{f1} = \mu_1 F \tag{1}$$

Where, μ_1 is the coefficient of friction at the roller-shaft interface and F is the grasp force.

The friction force between the roller and the object prevents roller slippage on the object surface and is given by

$$F_{f2} = \mu_2 F \tag{2}$$

Where, μ_2 is the coefficient of friction at the roller-object interface.

The net torque at the roller-shaft interface is given by

$$T_{net} = F_{f2} r_2 - F_{f1} r_1, \qquad F_{f1} \leq mg \tag{3}$$

Where, T_{net} represents the tangential force during grasping. Slippage at the shaft-roller interface will begin when the net torque $T_{net} > 0$.

When both friction rollers are holding the object, the weight of the object will be shared between the two rollers such that each roller will support $\frac{1}{2}mg$. In general, a smaller net torque T_{net} will require a smaller grasp force to prevent slippage at the roller-shaft interface. This simple design concept allows slippage between the roller and the manipulated object to be prevented reliably.

3 TORQUE (TANGENTIAL FORCE) SENSOR DESIGN

The prototype parallel gripper incorporates two sensing elements, one for tangential force sensing and one for slippage sensing, each fitted to a parallel gripper jaw. The torque sensing element (Figure 2) is fitted with a full Wheatstone bridge torque sensor that senses the tangential force developed on the shaft by the weight of the object held in the gripper.

The roller rotates on the shaft, which in turn is supported on roller bearings at its two ends to minimise friction and allow the full torque that is developed on the roller by the object to be sensed by the torque pin that is bolted to the support.

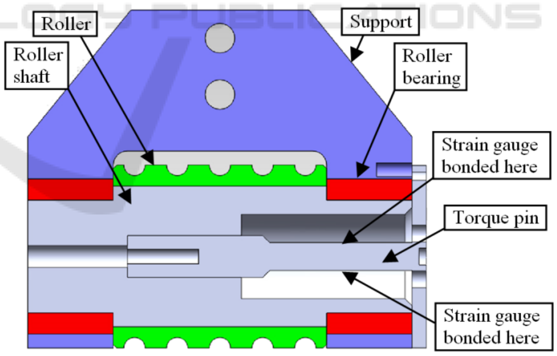

Figure 2: Cross-section through the torque sensing element assembly.

The TML QFCT-2 strain gauges used for the torque pin's full Wheatstone bridge have the following parameters:

- Gage factor GF = 2.12 +/-1 %
- Grid length = 2 mm
- Allowable strain = 3 %

The 3 % strain allows a strain gauge elongation of

$$2\text{ mm} * 0.03 = 0.06\text{ mm} = 60\ \mu\text{m}$$

Due to the very small values, strain is also expressed in "microstrain" (strain * 10^6). In this case the 3 % strain limit of the strain gauge can be expressed as

$$0.03 * 10^6 = 30{,}000 \text{ microstrain}$$

The torque pin (Figure 3) was designed to maximise its torsional strain when a 300 gram load is held in the gripper. It is made of 6061-T6 aluminium, has a diameter of 4 mm and a length of 20 mm. The design intent was to make the pin diameter as small as possible to maximise its strain under the given load (and therefore the torque resolution) but still allow the strain gauges to be fitted on its circumference without overlap.

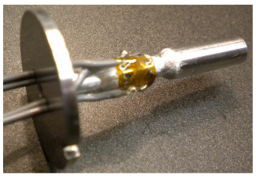

Figure 3: Torque pin assembly fitted with a full Wheatstone bridge.

The maximum torque strain for a round shaft is given as

$$\gamma_{\max} = \frac{4T}{\pi * E * R^3}(1 + \upsilon) \qquad (4)$$

Where,

γ_{max} - maximum shaft torsional strain
T - Applied torque to shaft
E – Elastic modulus of shaft material
R – Shaft (pin) outer radius
υ – Poison ratio

The design parameters for the torque pin are as follows:

$T = 3\ N * 0.013\ m = 0.039\ Nm$
$E = 68.9 * 109\ N/mm^2$
$R = 0.002\ m;$
$\upsilon = 0.33$

Substituting the parameters in equation 4 gives

$$\gamma_{\max} = \frac{4*0.039}{\pi*68.9*10^9*0.002^3}*(1+0.33)*10^6 = 120 \text{ microstrain}$$

The 120 microstrain range is well within the allowable 30,000 microstrain that can be applied to the strain gauge without causing it damage.

The theoretical full bridge output, not accounting for losses is estimated as

$$\frac{E_o}{E_i} = \frac{GF * \gamma_{\max}}{2} \qquad (5)$$

Where,

E_0 - bridge output (mV)
E_i - bridge excitation (V)
GF – the gauge factor of the strain gauge

Substituting in equation 5 gives a bridge output of

$$\frac{E_o}{E_i} = \frac{2.12 * 120 * 10^{-6}}{2} = 0.127\frac{mV}{V}$$

At full strain and an excitation voltage of 5 V DC the theoretical bridge output is

$$\frac{E_o}{E_i}@5\ V = 0.127\frac{mV}{V}5\ V = 0.635\ mV$$

The bridge output is expected to vary from the theoretical value due to variations in excitation voltage, variations in strain gauge extension wire resistance and because the strain gauge is not matched to aluminium for temperature compensation. These variations from the theoretical output will be relatively small (within 5 %), therefore acceptable for measuring the tangential force developed by the object on the robot gripper.

4 SLIPPAGE SENSOR DESIGN

The second jaw of the slippage sensing device was fitted with an incremental rotary encoder designed to sense roller rotation when the object slips in the gripper. In this design the steel roller support shaft is press-fitted into the aluminium roller such that they rotate together. The shaft can rotate in the steel plain bearings (Figure 4). The encoder is attached to the support using a screw, and its shaft is coupled to the roller support shaft via a silicone rubber disc. This allows the encoder to sense relative motion between the roller support shaft and the steel plain bearings, therefore allowing slippage to be detected by the same principle as described in section 2 above.

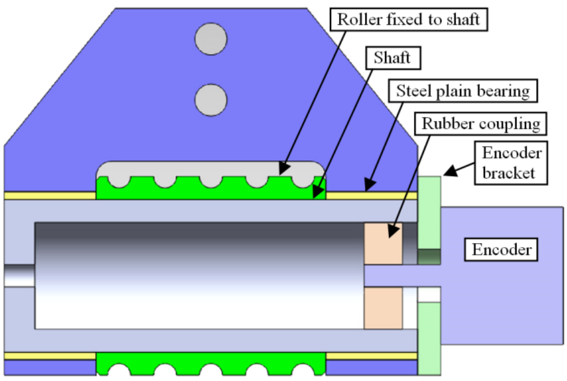

Figure 4: Cross-section through the slippage sensing element assembly.

5 EXPERIMENTAL SETUP

The major components of the experimental setup are shown in Figure 5 to Figure 9. The schematic representation of the experimental setup is shown in Figure 10.

Figure 5: Friction-based tangential force sensing device fitted with torque sensor.

Figure 6: Nemicon 18S-500-2MC-2-15-00E incremental encoder, used as slippage sensor.

Friction-based slippage sensing roller assembly is fitted with the Nemicon incremental encoder. The rubber O-rings are used to increase the coefficient of friction and provide mechanical compliance between the gripper and the grasped object. The O-rings also increase resistance to object rotation in the gripper due to the discrete contact points formed with the object (Dzitac et al., 2014).

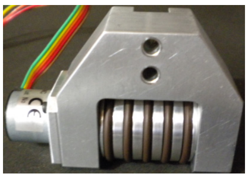

Figure 7: Encoder fitted to the roller assembly.

The Windows 7 operating system, running on an Asus notebook and executing custom vision software, processes the image received from the Basler vision camera to determine object shape, size, location and orientation. Object data is sent to the Moacon controller via an RS232 communication link. The Moacon C programmable controller (with digital inputs, relay outputs, analog inputs, quadrature encoder inputs, pulse width modulation PWM outputs and four position controllers for the XYZ and R stepper motor drivers) runs custom software that performs signal processing, motion planning, instinctive control, motion control and robot control at a basic level.

Figure 8: Moacon controller.

XYZ+R Cartesian robot ("R" stands for gripper rotation around Z axis) fitted with a modified Schunk RH701 electric gripper to allow higher grasp forces to be applied. This allows a 300 g object to be held safely without overstressing the gripper.

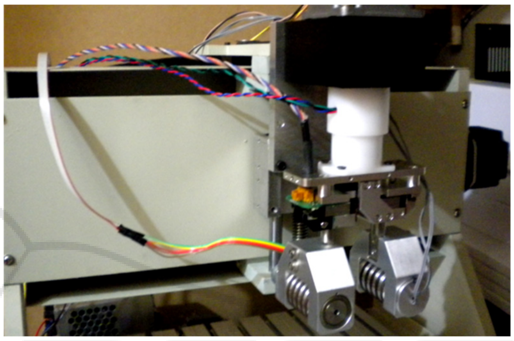

Figure 9: Cartesian robot fitted with gripper, slippage sensing element and tangential force sensing element.

Other experimental setup components include the:

- Full bridge amplifier model TWL-9R92 for torque sensor strain gauges;
- G251X digital stepper motor driver for XYZ and R axes;
- MD10C brush motor PWM drive for grasp force control.

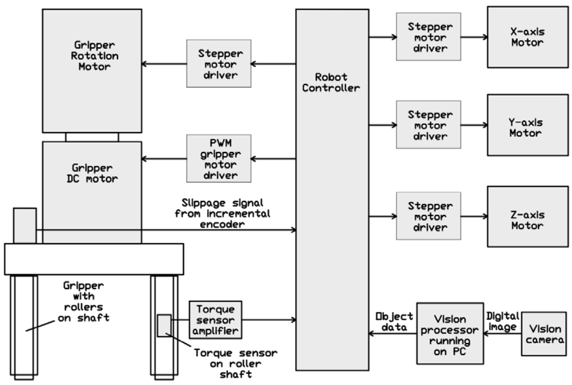

Figure 10: Schematic representation of the experimental setup using the final friction-based gripper design – the vision camera is used to find the object.

Three sets of experiments were conducted to assess different slippage control strategies:

- Experiment 1 – Simple slippage control;
- Experiment 2 – Sensor fusion based slippage control;
- Experiment 3 – Proportional based slippage control.

A 300 gram aluminium object was used for the experiment (Figure 11). The robot was instructed to execute the following tasks autonomously:

- Grasp the object with approximately 10 % of the available grasp force;
- While lifting the object, adjust the grasp force to stop slippage;
- When object lifting is completed accelerate the gripper downward then upward and monitor/control slippage;
- If slippage becomes large and potentially uncontrollable (i.e. there is not enough grasp force available to control slippage), stop robot motion and revert to manual robot control by a human to prevent damage;
- Else move gripper down and release the object.

Constraints and assumptions:

- Object shapes were limited to rectangular and cylindrical;
- Object mass was limited to approximately 300 grams to avoid overstressing the gripper;
- The object was assumed to be capable of sustaining 100 % grasp force without damage;
- The roller was assumed to always rotate when object slippage occurred. The term "object slippage" is used here to mean slippage at the roller-shaft interface not at the roller-object interface;

  Initial grasp force creates sufficient contact with the object to cause the roller to rotate when object lifting begins.

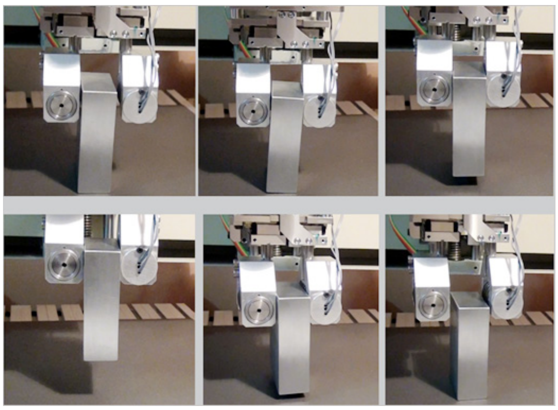

Figure 11: Object grasping, lifting and releasing sequence using the prototype slippage and tangential force sensing device.

5.1 Experiment 1 Results – Simple Slippage Control

The simple slippage control strategy requires the robot to apply an initial grasp force of 10 % and then increment the grasp force by 5 % when slippage is detected. Grasp force is estimated from the percentage of the pulse width modulated (PWM) current applied to the gripper motor. Figure 12 shows the grasp force, tangential force and slippage sensing encoder pulses recorded during the grasp and manipulation cycle using this control strategy.

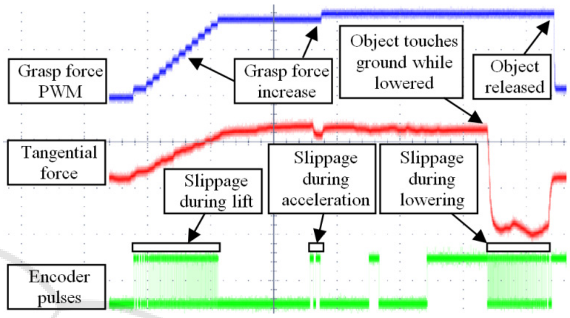

Figure 12: Initial grasp force set at 10 % of range. Grasp force increments are in steps of 10 %. The oscilloscope horizontal time scale is 2 s/division. Slip during acceleration is about 0.25 mm (i.e. roller rotates 1.44 ° on its Ø20 mm support shaft).

Unpredicted slippages were recorded in each of the ten object manipulation attempts. However, all unpredicted slippages were successfully resolved by increasing the grasp force and stopping the slippage, partially due to the medium manipulation velocity of approximately 1 m/s.

The results for the simple slippage control strategy are summarised in Table 1.

Table 1: Results for simple slippage control strategy.

Total object lifts	Unpredicted slippage	Slippage stopped successfully
10	10	10

5.2 Experiment 2 Results – Sensor Fusion Slippage Control

This experiment was conducted using the same hardware, methodology and constraints as in Experiment 1 above, except that the "sensor fusion" slippage control strategy (Dzitac et al., 1014) was used here. The diagram in Figure 13 illustrates the grasp force control algorithm used; sensor fusion determines whether slippage is "potential", "controllable" or "potentially uncontrollable". The recorded grasping and manipulation data is shown in Fig. 14.

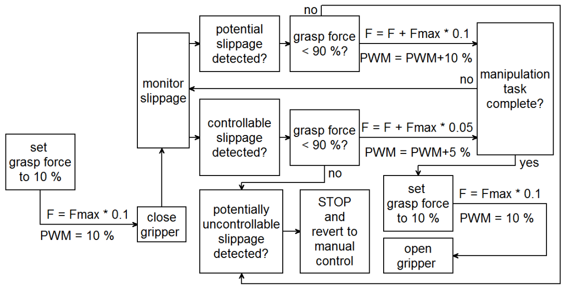

Figure 13: Grasp force control state diagram including sensor fusion based slippage detection.

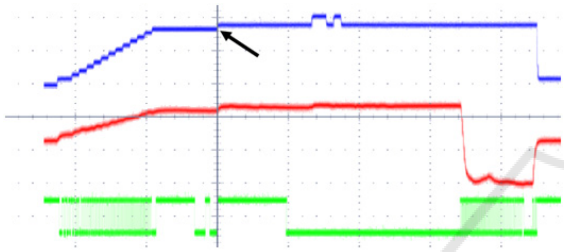

Figure 14: Unpredicted slippage occurred during lifting but was stopped by increasing grasp force.

Table 2 summarises the experimental results. One unpredicted slippage occurred during the initial lift of the first attempt. Two unpredicted slippages also occurred due to a "creep" effect noticed during experimentation. Because the encoder tracks the roller displacement over time, small slippages accumulate until it is sufficient to trigger a slippage event, which is defined as > 4 encoder counts. This behaves like a slippage integrator; however when a slippage event is triggered as a result of slippage creep, the grasp force increase stops slippage, but the sensor fusion strategy in its current form cannot predict the slippage because the changes in tangential force are too small to trigger a controller reaction.

Table 2: Results for sensor fusion slippage control strategy.

Total object lifts	Unpredicted slippage	Slippage due to "creep"	Slippage prevented successfully
10	1	2	7

5.3 Experiment 3 Results – Proportional Slippage Control

This experiment was conducted using the same hardware, methodology and constraints as in Experiments 1 and 2 above, except that the performance of a modified version of the slippage control strategy was compared to the performance of the sensor fusion grasp force control strategy.

This strategy uses the ratio of the static to the dynamic coefficient of friction $\frac{\mu_s}{\mu_k}$ as a scaling factor for grasp force correction that depends on the values of the two coefficients of friction at the roller-shaft interface where slippage occurs first. The reasoning behind this strategy is that the additional grasp force required to stop "object slippage" (i.e. slippage at the roller-shaft interface) will be proportional to the $\frac{\mu_s}{\mu_k}$ ratio at the roller-shaft interface and can be illustrated as follows.

Let $\mu_k F_1$ in Figure 15 be the grasp force at which slippage stops during object lifting and $\mu_s F_1$ the static friction force when slippage stops. If the grasp force is then reduced to the point of incipient slippage (i.e. the natural grasp force safety margin $F_{SM} = 0$), the reduced static friction becomes $\mu_s F_2$ and results in the following relationship

$$\mu_k F_1 = \mu_s F_2 \tag{6}$$

Re-arranging gives

$$F_1 = F_2 \left(\frac{\mu_s}{\mu_k}\right) \tag{7}$$

Therefore, at the instant when slippage starts F_2 (i.e. the grasp force) has to be increased by at least the $\frac{\mu_s}{\mu_k}$ ratio to stop slippage successfully.

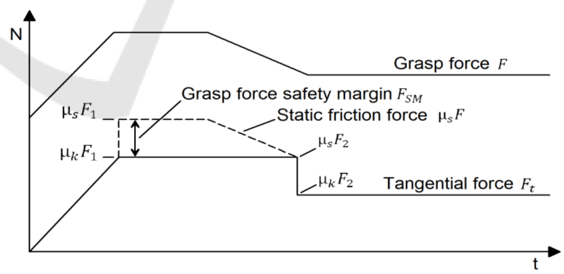

Figure 15: Grasp force reduction to the point of roller slippage on shaft.

The proposed grasp force control strategy in this case (when no slippage takes place) can be expressed as follows

$$F = F_1\left(1 + \left(\frac{|F_{t1} - F_t|}{F_{t1}}\right)\right), F_{t1} > 0 \tag{8}$$

Where,

- F is the total grasp force applied to the object;

- F_1 is the grasp force recorded at the point where slippage stopped while lifting the object; it is the static component of the total grasp force;
- F_{t1} is the tangential force recorded at the point where slippage stopped while lifting the object;
- F_t is the current tangential force developed by the grasped object on the roller;
- $|F_t - F_{t1}|$ is the absolute value of the tangential force change;
- $F_1\left(\frac{|F_{t1}-F_t|}{F_{t1}}\right)$ is the dynamic component of the total grasp force; its value changes in proportion to changes in F_t relative to F_{t1}.

When slippage signals are detected, the static component F_1 is assigned a new value that has been incremented by a factor $\frac{\mu_s}{\mu_k}$, which allocates a grasp force safety margin proportional to the friction characteristics at the roller-shaft interface. This increases the static components of the grasp force safety margin to prevent future slippage and can be expressed as follows

$$F_{1_{new}} = F_1\left(\frac{\mu_s}{\mu_k}\right) \quad (9)$$

The grasp force control in equation 8 can also be expressed in terms of PWM duty as follows

$$PWM = PWM_1\left(1 + \left(\frac{|F_{t1} - F_t|}{F_{t1}}\right)\right), F_{t1} > 0 \quad (10)$$

Where,

- PWM is the pulse width modulation duty applied to the gripper motor; it controls the grasp force of the gripper;
- PWM_1 is the pulse width modulation recorded at the point where slippage stopped while lifting the object;
- $PWM_1\left(\frac{|F_{t1}-F_t|}{F_{t1}}\right)$ is the dynamic component of the total grasp force; its value changes in proportion to changes in F_t relative to F_{t1}.

When slippage is detected, PWM_1 will be assigned a new value that has been increased by the $\frac{\mu_s}{\mu_k}$ factor as follows

$$PWM_{1_{new}} = PWM_1\left(\frac{\mu_s}{\mu_k}\right) \quad (11)$$

Equation 11 is useful because most controllers are equipped with PWM outputs that can be used to control the grasp force of a robot gripper.

To improve the initial grasp-lift time and the overall reaction to slippage, a rate-based grasp force safety margin control strategy was used as a replacement for equation 11. When slippage is detected PWM_1 is increased based on the rate of received encoder pulses (i.e. rate of slippage).

$$PWM_{1_{new}} = PWM_1 + ks \quad (12)$$

Where,

- k is a gain constant and s is the slippage rate within a control loop cycle (e.g. number of encoder pulses in 100 ms).

This rate-based slippage control is possible because the rate of slippage is readily available from the rate of the encoder pulses generated during slippage.

The recorded grasping and manipulation data is shown in Figure 16.

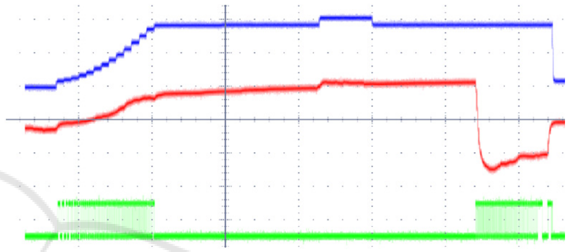

Figure 16: Slip-rate based control during initial lifting and "proportional" control after initial lifting.

Table 3 summarises the experimental results for the rate-based grasping and manipulation experiment.

Table 3: Results for proportional slippage control strategy.

Total object lifts	Unpredicted slippage	Slippage due to "creep"	Slippage prevented successfully
10	2	2	6

6 CONCLUSION AND FUTURE WORK

The addition of torque sensing to one gripper roller made it possible to use preventive slippage control strategies such as sensor fusion and proportional control, which is not possible when using a slippage sensor alone.

The slippage prevention strategies based on sensor fusion and proportional control used in these experiments perform better that basic slippage control strategy that increases grasp force after slippage is detected. However, unpredicted slippage still occurred due to the "slippage creep" effect inherent in the current design. An unpredicted slippage is considered to be a slippage event to which the control strategy did not react before the actual slippage was detected.

The current tangential force sensing prototype is affected by hysteresis due to stray friction in the mechanical assembly. Future work could be done to reduce or eliminate stray friction.

A derivative term could be added to the proportional term of the proportional controller to facilitate reaction to tangential force rate of change, and as a result improve slippage prevention.

The developed slippage detection and control strategy can sense slippage and tangential force in one axis only. Further work can be done to add slippage sensing in other axes.

The slippage control strategy presented here is not a generic solution for slippage control in robotic object manipulation, but is rugged, reliable, repeatable and highly customizable.

REFERENCES

Tremblay M. R., Cutkosky M. R., 1993. “Estimating Friction Using Incipient Slip Sensing During a Manipulation Task,” In *Proceedings of IEEE International Conference on Robotics and Automation*, Atlanta (GA).

Bowden F. P., Tabor D., 1986. *The Friction and Lubrication of Solids*, UK: Oxford Science Press.

Petchartee S., Monkman G., 2007. “Pre-slip detection based Tactile Sensing,” In *Proceedings of International Conference on Sensors*, Sensor Networks and Information, Toulouse.

Mingrino A., Bucci A., Magni R., Dario P., 1994. “Slippage Control in Hand Prostheses by sensing Grasping Forces and Sliding Motion,” In *Proceedings of the IEEE/RSJ International Conference on Intelligent Robots and Systems*.

Canepa G., Campanella M., Rossi D., 1994. “Slip Detection by a Tactile Neural Network,” In *Proceedings of IEEE/RSJ Internationl Conference on Intelligent Robots and Systems*.

Pelossof R., Miller A., Allen P., Jebara T., 2004. “An SVM Learning Approach to Robotic Grasping,” In *Proceedings of International Conference on Robotics and Automation*.

Dubey V. N., Crowder R. M., 2006. “A dynamic tactile sensor on photoelastic effect,” *Sensors and Actuators*, no. 128, pp. 217-224.

Watanabe N., Obinata G., 2007. “Grip Force Control Based on the Degree of Slippage Using Optical Tactile Sensor,” In *International Symposium on Micro-NanoMechatronics and Human Science*.

Abdo J., Tahat M., Abouelsoud A. A., 2009. “The effect of excitation frequencies on stick-slip amplitude,” In *Proceedings of International Conference on Integrity, Reliability and Failure*, Porto (Portugal).

Russel R. A., 1990. Robot Tactile Sensing, New York: Prentice Hall.

Choi B., Cho H. Kang R., S., 2005. “Development of tactile sensor for detecting contact force and slip,” In *Proceedings of IEEE/RSJ International Conference on Intelligent Robots and Systems*, Edmonton.

Rossiter J., Mukai T., 2005. “A Novel Tactile Sensor Using a Matrix of LEDs Operating in Both Photoemitter and Photodetector Modes,” In *Proceedings of 2005 IEEE Conference on Sensor*.

Dahiya R. S., Metta G., Valle M., Sandini G., 2010. “Tactile Sensing - From Humans to Humanoids,” *IEEE Transactions on Robotics*, vol. 26, no. 1.

Dzitac P., Mazid A. M., 2012. “A method to control grip force and slippage for robotic object grasping and manipulation”, In *MED 2012 Proceedings of the Control and Automation Mediterranean conference*, Barcelona, Spain. pp. 116-121.

Dzitac P., Mazid A. M., Littlefair G., Polishetty A., 2014. “The Effective Radius and Resistance to Slippage”, In Proceedings of the 11th International Conference on *Informatics in Control, Automation and Robotics* (ICINCO 2014), Vienna, Austria.

Dzitac P., Mazid A. M., Littlefair G., Polishetty A., 2014. “Robotic Grasping and Manipulation Controller Framework - Architecture Redevelopment”, In *Proceedings of the 11th International Conference on Informatics in Control, Automation and Robotics* (ICINCO 2014), Vienna, Austria.